

**UNITED STATES OF AMERICA
BEFORE THE
FEDERAL ENERGY REGULATORY COMMISSION**

Electric Storage Participation in Markets)	Docket Nos.	RM16-23-000
Operated by Regional Transmission)		AD16-20-000
Organizations and Independent System Operators)		

**COMMENTS OF DRs. AUDUN BOTTERUD, APURBA SAKTI, AND FRANCIS
O’SULLIVAN, MASSACHUSETTS INSTITUTE OF TECHNOLOGY,
REGARDING PROPOSED RULEMAKING
ON ELECTRIC STORAGE PARTICIPATION IN MARKETS¹**

Pursuant to 18 CFR Part 35, Drs. Audun Botterud, Apurba Sakti, and Francis O’Sullivan respectfully submit these comments in response to the Federal Energy Regulatory Commission’s (“FERC” or “Commission”) Notice of Proposed Rulemaking (“NOPR”) issued on November 17, 2016 in the above-dockets on Electric Storage Participation in Markets Operated by Regional Transmission Organizations and Independent System Operators.

I. Introduction

The Comments have been prepared by, and reflect the research and recommendations of (1) Dr. Audun Botterud, who is a Principal Research Scientist in the Laboratory for Information and Decision Systems at MIT. The main goal of Dr. Botterud’s research is to improve the understanding of the complex interactions between engineering, economics, and policy in electricity markets, including by integrating energy storage into a smarter electricity grid. Dr. Botterud is also a Principal Energy Systems Engineer at Argonne National Laboratory. Some of the research referred to in this response originates from a research project conducted at Argonne

¹ These submitted comments exclusively reflect the collective views of Drs. Audun Botterud, Apurba Sakti, and Francis O’Sullivan who are researchers at the Massachusetts Institute of Technology (MIT). The comments expressed herein do not necessarily reflect the views of, and therefore should not be attributed to, the University or any Department thereof, or of Argonne National Laboratory.

National Laboratory; (2) Dr. Apurba Sakti, who is a Research Scientist at the MIT Energy Initiative. Dr. Sakti has worked on the design and cost of Li-ion batteries, and is focusing on different techno-economic aspects of energy storage systems at the grid-level as well as for applications in the transportation sector; and (3) Dr. Francis O’Sullivan is Director of Research and Analysis for the MIT Energy Initiative, and a Senior lecturer at the MIT Sloan School of Management. Dr. O’Sullivan’s work is focused on the evolution of the electric power sector, particularly on the integration of large-scale solar and wind resources, advanced storage deployment, and on how digitization is enabling operational optimization and unlocking new business models. The biographies of Drs. Botterud, Sakti, and O’Sullivan are attached.

II. Summary

We support the general purpose of the NOPR to remove market barriers for energy storage and distributed energy resources to allow for full participation in the organized electricity markets, including for capacity, ancillary services, and energy. We support the recommendation that participation models be established for these resources to recognize their physical and operational characteristics.

Creating an equal playing field for all electricity market participants is at the heart of FERC’s mission. The regulatory framework established by FERC therefore will be of critical importance for emerging technologies in the power grid like energy storage. For instance, in a recent study (Sakti et al. 2017) we show that a switch from hourly to 5-min settlements in the real-time market, as dictated by the recent FERC Order No. 825, will more than double the potential revenues that can be realized from energy storage arbitrage for a given location and time period. Adoption of this and other rules that recognize the unique characteristics of storage

technologies will enable for their optimal provision of services and values to the grid and also provide adequate market price signals necessary for their future deployment.

Our specific comments address the part of the NOPR that relates to energy storage, a subject in which we have extensive expertise, particularly as it pertains to its integration into electricity markets and the electric power grid. Our Comments are based, in part, on our recent paper “Enhanced Representations of Lithium-Ion Batteries in Power Systems Models and their Effect on the Valuation of Energy Arbitrage Applications” (Sakti et al. (2017)), which is attached to our Comments. Our Comments also draw upon other research on energy storage and electricity markets, conducted by ourselves and others.

III. Comments

A. Elimination of Barriers to Electric Storage Resource Participation in Organized Wholesale Electric Markets

1. Creating a Participation Model for Electric Storage Resources

26-32: We fully support the Commission’s proposal to require ISO/RTOs to establish a specific participation model for energy storage. As pointed out in the NOPR, energy storage has unique characteristics that differ from traditional supply and demand resources in electricity markets: the prime example being that energy storage is an energy-limited resource that can both sell and buy electricity from the grid. Hence, participation models developed for other resources are not likely to appreciate all the physical and operational constraints of electric storage. Moreover, a number of studies show how energy storage can provide multiple benefits to the grid, and that the associated value tends to increase as the penetration of renewable energy resources increases due to the power system’s need for greater flexibility (e.g. Denholm et al. 2010, Koritarov et al. 2014). Given this, establishing a participation model that enables energy storage to realize the multiple revenue streams that accrue from the set of services it provides to

the grid will establish a fair playing field for energy storage compared to other technologies. Putting in place such a participation model will support the expansion of grid-level storage technologies where they provide the most cost-effective solution. At the same time, we agree with the Commission that it is prudent to allow ISO/RTOs some flexibility in defining their own participation model and qualification requirements, so long as they comply with the overall goals of the NOPR. Such an approach will enable the implementation of rules that account for differences in regional characteristics and existing ISO/RTO market rules.

2. Requirements for the Participation Model for Electric Storage Resources

a. Eligibility to Participate in Organized Wholesale Electric Markets

48: We agree that the participation model should ensure that any participating resource can provide any capacity, energy, and ancillary service that it is capable of providing in the organized wholesale electric markets. This is of utmost importance to enable non-discriminatory access to the wholesale markets and an equal opportunity for energy storage technologies compared to other resources.

50: We agree that participation in ancillary services markets should be based on the resource's ability to provide such services within the required time frames rather than on the real-time operating status of the resource. For instance, for conventional generators, the ability to provide spinning reserves and regulation is directly linked to its real-time operating status (*i.e.* it needs to be generating to provide these services). In contrast, most storage technologies can provide these services regardless of the real-time commitment and dispatch status. It is still important to recognize individual differences between energy storage technologies. For instance, electrochemical batteries are usually very flexible in terms of ramp rates and fast switching between charging and discharging states, but with relatively short energy storage duration. In

contrast, pumped storage hydro plants may have reduced ability to dispatch across the full capacity range (particularly in pumping mode) and with some time delays between charging and discharging modes, but with longer storage duration.

51: We believe that for many energy storage technologies it is not necessary to have a (non-zero) energy schedule to provide certain ancillary services (pumped storage hydro may be an exception for reasons mentioned above). Batteries can quickly ramp up (discharge) or down (charge) from a zero power starting point. Given this two-way flexibility, a zero power output from a battery can be considered equivalent to a non-zero energy schedule for a conventional generating resource. The NOPR raises an interesting question about whether pricing of energy and ancillary services would continue to be internally consistent, in the case where a resource offers ancillary services without offering energy. We do not see internal inconsistencies under such a scenario. However, under the assumption that energy and reserves are co-optimized in the electricity market, the cleared schedule of the energy storage unit in the reserves market may depend on whether or not it offers energy, as this influences its opportunity cost as seen by the market clearing optimization algorithm. The structure of the energy storage offer (i.e. one or multiple products) may therefore also influence the overall market outcome. Still, the resulting market outcome would reflect resource costs and opportunity costs based on the offers provided to the energy and ancillary services markets, as long as energy and reserve schedules are co-optimized in the market clearing. In contrast, if energy and reserves markets are cleared separately, energy storage and other market participants must estimate opportunity costs individually and build that into their offers. This is complex problem, especially for an energy-limited resource like energy storage. We therefore believe that a market design based on co-optimization will provide better scheduling and pricing outcomes for energy storage.

As an example, in Li et al. (2016) we develop a unit commitment and economic dispatch model where battery energy storage can provide energy and operating reserves. The model co-optimizes energy and operating reserves for the system, taking resource offer costs as well as system opportunity costs into account. Energy storage is allocated to provide energy and/or operating reserves in different time periods, whatever minimizes the total cost of meeting energy demand and the system's operating reserve requirements. The resulting schedules include hours where the battery is scheduled to provide reserves (spinning reserves or regulation) without providing an energy schedule.

b. Bidding Parameters for Electric Storage Resources

66-68: We agree that bidding parameters should reflect and account for the physical and operational characteristics of electric energy storage. In this context, we would emphasize that for most electrochemical energy storage technologies this may also include adequate representation of battery power limits, efficiency/losses, and battery degradation. In particular, we show in Sakti et al. (2017) that power limits in Li-Ion batteries are a function of the state of charge (SOC) of the battery (as illustrated in figure 1b of the attached paper). Moreover, battery efficiency and energy losses are a function of both SOC and charge/discharge power as (illustrated in figure 1a of the attached paper). We develop a battery model that account for these relationships and show for an energy arbitrage application that they have substantial impact on the battery's dispatch schedule and revenues (i.e. up to 10% change in battery revenues). Hence, ideally bidding parameters for energy storage providers should enable a dynamic representation of power limits and efficiency losses as a function of SOC. In related work, we show in Wankmüller et al. (2017) that battery degradation is a critical issue for batteries that substantially impacts the lifetime economic value of the asset used in an energy arbitrage application.

Moreover, we show that reflecting degradation cost in offering strategies to reduce battery cycling contributes to substantially increase battery lifetime and economic viability. Hence, bidding parameters should also enable the representation of battery degradation and corresponding capacity fade, which may also be a function of SOC and power charge/discharge profiles. Additional bidding parameters (these may be optional) may therefore be required to fully represent the characteristics of electrochemical storage technologies.

The Commission recommends using SOC as a bidding parameter. It is not clear to us from the NOPR exactly what this means and how it would be applied. Should energy storage provide a desired SOC level at the beginning or end of the scheduling period? The Commission should clarify how SOC would be utilized. In this respect we would provide the observation that in order to make use of the full flexibility in energy storage resources, a fixed SOC target may not be a good solution since it limits the dispatch flexibility in real-time operations. We show in Li et al. (2016) that an SOC range is a better strategy to enable the use of the battery as a flexible resource to address unexpected system deviations in real-time.

69-70: We agree that the ISO/RTO, in principle, is in the best position to manage energy storage scheduling and SOC in order to minimize system costs. However, this is a challenging task, especially considering the increasing uncertainty associated with greater renewable resource penetration levels. Therefore, a key challenge is the development of unit commitment and economic dispatch strategies that make optimal use of the flexibility provided by energy storage. We believe that significant innovation will be needed to develop new scheduling and dispatch formulations that make optimal use of energy storage in unit commitment, economic dispatch, and market clearing. Ultimately, ISO/RTO scheduling software is not likely to reflect all technical and economic characteristics of energy storage technologies of concern for the

energy storage asset owners. We therefore agree that energy storage participants should have the option to manage SOC themselves, while recognizing that this includes exposure to any deviation penalties in line with other resources on the grid.

71: Substantial software changes are likely to be needed to introduce the bidding parameters proposed in the NOPR and discussed above. This may influence the computational efficiency of the market clearing optimization. There will always be a trade-off between computational efficiency and accuracy in representing technology constraints. In implementing improved model representations of energy storage, the benefits need to be weighed against alternative software improvements to address other needs in the system.

c. Eligibility to Participate as a Wholesale Seller and Wholesale Buyer

81: We support the proposed requirement that electric storage resources can be dispatched and set the wholesale market clearing price as both a wholesale seller and wholesale buyer. It is important that the economic preferences of energy storage are reflected in the market clearing when storage assets operate as load as well as supply resources. This will also enable efficient use of energy storage's flexibility in system operation. However, we also agree that energy storage should have the option to self-schedule, in line with other load resources in the grid.

83: We agree that simultaneous participation as supply and demand resources is necessary in order to make full use of the flexibility provided by energy storage in system operation. The optimal mode of operation for energy storage (supply vs. demand) to minimize system cost cannot be determined up front. On the issue of the possibility of conflicting dispatch signals, we offer the suggestion that this could also be avoided by building logical checks into

the market clearing algorithm that prevents energy storage supply offers and demand bids from the same energy storage resource to be accepted at the same time.

e. Energy Used to Charge Electric Storage Resources

100: We agree that the same price signal should apply to energy storage when it buys and sells electricity from the wholesale market, and that the LMP represent a just and reasonable rate in both cases. The LMP reflects the marginal value of electricity at a given location and therefore provides the correct incentive for the dispatch of energy storage resources.

IV. Correspondence

All correspondence or communications concerning these comments should be addressed to the following:

Dr. Audun Botterud
Laboratory for Information and Decision Systems
Massachusetts Institute of Technology
77 Massachusetts Ave, 32-D632
Cambridge, MA 02139
audunb@mit.edu

Dr. Apurba Sakti
MIT Energy Initiative
Massachusetts Institute of Technology
77 Massachusetts Ave, E19-308
Cambridge, MA 02139
sakti@mit.edu

Dr. Francis O'Sullivan
MIT Energy Initiative
Massachusetts Institute of Technology
77 Massachusetts Ave, E19-370Q
Cambridge, MA 02139
frankie@mit.edu

V. Conclusion

We support the general purpose of the NOPR to remove market barriers for energy storage to allow for full participation in the organized electricity markets, including for capacity, ancillary services, and energy. We respectfully request the Commission to consider these comments in proceeding with the proposed rulemaking.

Respectfully Submitted,

Audun Botterud

Apurba Sakti

Francis O'Sullivan

February 13, 2017

Brief Biographies of Drs. Audun Botterud, Apurba Sakti, and Francis O’Sullivan

Audun Botterud

Audun Botterud is a Principal Research Scientist in the Laboratory for Information and Decision Systems at MIT. The main goal of his research is to improve the understanding of the complex interactions between engineering, economics, and policy in electricity markets. He is particularly interested in integration of renewable energy and energy storage into a smarter electricity grid. Towards this end, he uses analytical methods from operations research and decision science combined with fundamental principles of electrical power engineering and energy economics. Dr. Botterud is also a Principal Energy Systems Engineer at Argonne National Laboratory. He received his MSc in Industrial Engineering and PhD in Electrical Power Engineering from the Norwegian University of Science and Technology.

Apurba Sakti

Apurba Sakti is a Research Scientist at the MIT Energy Initiative, and was previously a Postdoctoral Associate in the MIT Department of Chemical Engineering. Prior to MIT, Dr. Sakti was a graduate research assistant in the Vehicle Electrification Group at Carnegie Mellon University while completing his Ph.D. in Engineering and Public Policy. For his doctoral dissertation, Dr. Sakti worked on the design and cost of Li-ion batteries and the associated public policy implications for personal vehicle electrification. His work has since been mentioned in the New York Times and is also being used by a start-up to improve battery manufacturing. Dr. Sakti has experience working with the United Nations Development Programme in Zagreb and the American Council for an Energy Efficient Economy in Washington, D.C. At MIT, Dr. Sakti is focusing on different techno-economic aspects of energy storage systems at the grid-level as well as for applications in the transportation sector.

Francis O’Sullivan

Francis O’Sullivan is Director of Research and Analysis for the MIT Energy Initiative, and a Senior lecturer at the MIT Sloan School of Management. His work is focused on the evolution of the electric power sector, particularly on the integration of large-scale solar and wind resources, advanced storage deployment, and on how digitization is enabling operational optimization and unlocking new business models. He was a Senior Advisor to the US Department of Energy’s 2017 Quadrennial Energy Review, and is a member of the National Academies’ Roundtable on Science and Technology for Sustainability. Dr. O’Sullivan is also a Senior Associate with the Energy and National Security Program at the Center for Strategic and International Studies. Frank is an electrical engineer by training, receiving his Ph.D., E.E., and S.M. degrees from the Massachusetts Institute of Technology, and his B.E. degree from the National University of Ireland.

References

- Denholm P., Ela E., Kirby B., Milligan M., “The role of energy storage with renewable electricity generation,” Technical Report NREL/TP-6A2-47187, National Renewable Energy Laboratory, Golden, CO, January, 2010.
- Koritarov V., Veselka T., Gasper J., Bethke B., Botterud A., Wang J., Mahalik M., Zhou Z., Milostan C., Feltes J., Kazachkov Y., Guo T., Liu G., Trouille B., Donalek P., King K., Ela E., Kirby B. Krad I, Gevorgian V., “Modeling and Analysis of Value of Advanced Pumped Storage Hydropower in the United States,” Technical Report ANL/DIS-14/7, Argonne National Laboratory, Argonne, IL, June 2014.
- Li N., Uckun C., Constantinescu E., Birge J.R., Hedman K.W., Botterud A., “Flexible Operation of Batteries in Power System Scheduling with Renewable Energy”, *IEEE Transactions on Sustainable Energy*, Vol. 7, No. 2, pp. 685-696, 2016.
- Sakti A., Gallagher K.G, Sepulveda N., Uckun C, Vergara C., de Sisternes F., Dees D.W., Botterud A., “Enhanced representations of lithium-ion batteries in power systems models and their effect on the valuation of energy arbitrage applications,” *Journal of Power Sources*, Vol. 342, pp. 279-291, 2017.
- Wankmüller F., Thimmapuram P., Gallagher K.G., Botterud A., “Impact of Battery Degradation on Energy Arbitrage Revenue of Grid-level Energy Storage,” *Journal of Energy Storage*, Vol. 10, pp. 56-66, 2016.



Enhanced representations of lithium-ion batteries in power systems models and their effect on the valuation of energy arbitrage applications



Apurba Sakti^{a, *}, Kevin G. Gallagher^b, Nestor Sepulveda^a, Canan Uckun^c,
Claudio Vergara^a, Fernando J. de Sisternes^d, Dennis W. Dees^b, Audun Botterud^{a, c, **}

^a MIT Energy Initiative, Massachusetts Institute of Technology, Cambridge, MA 02139, USA

^b Chemical Sciences and Engineering Division, Argonne National Laboratory, 9700 S. Cass Avenue, Argonne, IL 60439, USA

^c Energy Systems Division, Argonne National Laboratory, 9700 S. Cass Avenue, Argonne, IL 60439, USA

^d The World Bank, 1850 I St. NW, Washington DC 20433, USA

H I G H L I G H T S

- We develop three enhanced mixed integer-linear representations of li-ion batteries.
- We investigate the effect of 5-min vs. a 60-min price signals on arbitrage profitability.
- Profits are overestimated by up to 10% when power limits and losses are constant.
- Profits improve by up to 60% with 5-min price signals compared to hourly prices.

A R T I C L E I N F O

Article history:

Received 10 September 2016

Received in revised form

7 December 2016

Accepted 15 December 2016

Keywords:

Enhanced battery representation

Li-ion MILP models

Power systems arbitrage modeling

Real-time pricing effects

A B S T R A C T

We develop three novel enhanced mixed integer-linear representations of the power limit of the battery and its efficiency as a function of the charge and discharge power and the state of charge of the battery, which can be directly implemented in large-scale power systems models and solved with commercial optimization solvers. Using these battery representations, we conduct a techno-economic analysis of the performance of a 10 MWh lithium-ion battery system testing the effect of a 5-min vs. a 60-min price signal on profits using real time prices from a selected node in the MISO electricity market. Results show that models of lithium-ion batteries where the power limits and efficiency are held constant overestimate profits by 10% compared to those obtained from an enhanced representation that more closely matches the real behavior of the battery. When the battery system is exposed to a 5-min price signal, the energy arbitrage profitability improves by 60% compared to that from hourly price exposure. These results indicate that a more accurate representation of li-ion batteries as well as the market rules that govern the frequency of electricity prices can play a major role on the estimation of the value of battery technologies for power grid applications.

© 2016 Elsevier B.V. All rights reserved.

1. Introduction

Widespread grid-level integration of variable renewable energy sources, such as solar and wind power, requires a power system capable of utilizing these resources efficiently. This in turn requires

other grid elements or mechanisms that can respond quickly to the variable and uncertain output of renewables in order to meet electricity demand instantaneously, increasing the overall “flexibility” of the system. Electrochemical energy storage systems (EESSs)—such as lithium-ion batteries— can contribute to increasing the power system’s flexibility in addition to providing a host of other services aimed at guaranteeing the power systems’ security of supply—e.g., system adequacy, voltage control, and different types of operating reserves and other ancillary services [1]. It is no surprise that the demand for advanced EESSs grew by

* Corresponding author.

** Corresponding author. Energy Systems Division, Argonne National Laboratory, 9700 S. Cass Avenue, Argonne, IL 60439, USA.

E-mail addresses: sakti@mit.edu (A. Sakti), abotterud@anl.gov (A. Botterud).

200% [2] in 2015—the largest annual deployment on record—and is forecast to grow substantially over the coming years as power systems reduce their carbon footprint by increasing the capacity of variable renewable resources. Decision support models for the power system address a range of issues from short-term operations to long-term planning of electricity supply, demand, and transmission. It is becoming common to consider the role of EESSs in these models, particularly in the context of renewable integration. For instance, from a system operations perspective, EESSs have been included in unit commitment and economic dispatch analysis in several recent studies [3–5]. The role of EESSs is also considered in longer-term generation expansion planning models [6,7]. A more specific application of EESSs is energy arbitrage, i.e. trading energy from the EESS in the electricity market to exploit temporal price differences, and several recent papers focus on this problem [8–10]. Power systems optimization models typically include a large number of variables and constraints to represent the physics and economics of the power grid and its components, and are usually formulated as mixed integer linear programming (MILP) problems. The traditional approach used in recent studies assessing the economic performance of EESSs using power systems models has been to adopt simple formulations to represent the storage capability limiting the representation of the nonlinear nature of the physical behavior of EESSs [6,7,11–14]. Simplistic representations of EESSs in power systems models typically include fixed roundtrip efficiencies or fixed rated power regardless of the charge/discharge levels and state of charge (SOC). Nevertheless, in reality these parameters are dependent on the EESS's power output/input as well as the EESS's state of charge. Ignoring these relationships misrepresents the behavior of the EESS and might lead to suboptimal modeling results as well as misleading assessments of the economic benefits and viability of EESSs.

When looking at the value proposition of EESSs, a prerequisite is that energy storage must be allowed to competitively participate in the electricity market, based on efficient price signals for all the different services it provides. Towards this end, market access and pricing frequency are two fundamental elements to increase the efficiency of a grid that is evolving as more renewable and distributed resources become part of it [15]. Market rules affecting EESSs are evolving accordingly, with one important example in the United States being the recent FERC ruling order. No 825 [16] requiring all market operators to use the same time interval for pricing and dispatch. In the case of several large electricity markets in the United States, including the Midcontinent Independent System Operator (MISO), this will move the financial settlements in the real-time energy market to 5-min prices instead of the hourly time resolution used so far. This change in market rules may have important implications for EESS, since energy arbitrage is the largest potential application for battery technologies and therefore represents a major market opportunity for investors in EESS.

In this paper, we develop a novel enhanced mixed integer-linear program (MILP) representation of the behavior of one type of EESS—a lithium-ion (NMC) battery pack— that includes all the inter-relationships between rated output, state-of-charge, and losses. The general representation can also be applied to other types of batteries. The proposed EESS formulation can be directly exported to a range of different power systems models based on MILP formulations. We test the applicability of the proposed EESS formulation with an energy arbitrage model that maximizes the profits from the lithium-ion battery pack that buys and sells energy from the grid, using price data from the MISO market. In particular, we assess the impact of using the enhanced representation of lithium-ion batteries on the optimal battery dispatch solution as well as the estimated profitability from energy arbitrage. Moreover, we use the energy arbitrage model with the enhanced ESS

representation to investigate the effect of a price signal that varies every 5-min compared to one that does so every 60-mins.

2. Methodological approach

A generic framework is proposed to capture the nonlinear physical phenomena that characterizes the behavior of EESSs and translates them into mixed integer-linear equations that can be included in traditional power systems models avoiding the excessive computational burden of introducing nonlinear equations in the model. The framework is then applied to model lithium-ion batteries, which were chosen for this exercise given their market dominance [17]. This framework enables the use of a single model to represent the primary behavior of many other battery chemistries by the specification of only a minimum of technology-specific parameters. This parametric model would be broadly applicable in the context of battery applications in power systems. Nevertheless, given that it uses one common parametric structure, it would likely be ill-suited for detailed studies focusing on the physical behavior of a given particular chemistry.¹

The approach taken in this work will improve the current treatment of EESSs in power systems models where the current battery representation is taken to the 0th order risking unphysical performance behavior. The improvement in accuracy resulting from a more realistic representation of EESSs is quantified by comparing the economic results derived from this new representation with those obtained from a generic (0th order) representation. For the purpose of this analysis we use a generic energy arbitrage application, but the proposed EESS model could also be incorporated into other power systems optimization models—e.g., unit commitment or capacity expansion— considering a wider range of EESS applications—e.g., operating reserves, black-start capabilities, voltage control. We first introduce the primary physics driving EESS and then develop detailed energy arbitrage model that incorporate this enhanced EESS representation.

2.1. Physical behavior of electrochemical energy storage systems (EESS)

The primary physics driving the behavior of EESS are described by thermodynamics, charge conduction, charge transfer at an interface, and mass transport. The system is assumed isothermal for this treatment. A mathematical model of the physical behavior of EESSs should therefore be consistent between these physical phenomena, which are discussed in more detail below. The equations modeling each of these phenomena are presented at the individual battery cell-level, which can be scaled up to represent values at the pack-level, comprising of a numerous individual cells for power system applications.

Thermodynamics— The open-circuit voltage (OCV) of an electrochemical cell is the difference in electrochemical potential between the negative and positive electrodes. The voltage of each electrode and thus the cell OCV is a function of the state-of-charge (SOC) of the battery. We define SOC here as the as fraction the Coulombic capacity of the battery in the charged state. The detailed physics that controls the OCV vs. SOC function are difficult to

¹ As each commercialized battery technology has already been subjected to intense modeling activities, the reader is referred to other works in the electrochemistry literature using empirical models focusing on the general energy balance of a battery system [18], the heat generation rate using the energy balance model [19], electrochemical-thermal modeling and experimental validation [20], and the simulation and optimization of lithium-ion battery systems [21] amongst others that involve detailed calculations for the internal electrochemical processes using physics-based models [22–26].

generalize or predict due to the complex and dynamic electrochemical phenomena involved. Indeed, first principle modeling activities, such as density functional theory, can capture the primary behavior of the OCV vs SOC function, but not the exact curve. Here we maintain a higher level view to capture the primary behavior. The Nernst equation, Eq (1), is an elementary expression of the OCV where the thermodynamic voltage, U , of an electrode is expressed as a function of the activity, a , of the reactants [27].

$$U_j = U_j^0 + \frac{RT}{nF} \ln \left(\frac{a_{ox}}{a_{red}} \right) \quad \text{for } j = n \text{ or } p \quad (1)$$

However, few battery electrodes follow the Nernst Equation, particularly in the most frequently recited form of Eq (1), which assumes unit activity coefficients (i.e., the activities are replaced with concentrations). Due to non-ideal interactions or the presence of multiple phases, most OCV vs SOC functions are not well represented on a log plot by a slope of RT/nF and often require a summation of several functional forms to precisely fit the observed behavior. In practice, engineers often fit an empirical function through the curve to achieve the highest fidelity in the fit [28–30]. We note that the activity or concentration of the oxidized species (subscript ox) and reduced species (subscript red) correspond to a specific SOC for the battery. Hereafter we use SOC as a non-dimensional form of the concentration of oxidized species in the positive electrode and reduced species in the negative electrode. The proposed framework is capable of using any empirical formulation, however, a general form of the OCV vs SOC function for the battery OCV (U) is shown in Eq. (2) as an example. The battery OCV is the difference between the OCV vs SOC functions for the positive and negative electrodes multiplied by the number of series connected cell groups. Here, the slope of the function may be modified with the parameter ξ . In one derivation for a single electrode, ξ is shown to be related to attractive or repulsive energetic interactions between reactants [31]. As Eq. (2) is an approximation of the battery voltage, ξ should be considered a fitting parameter. Eq. (2) can also include additional empirical fitting parameters (e.g. α and β) to capture the complex thermodynamics that govern the system. For example, layered oxide positive electrode materials in lithium-ion batteries have significant changes in the slope of the OCV vs SOC function. In addition, only a fraction of the total lithium content in layered lithium metal oxides is utilized. In that case, an effective SOC factor may be multiplied to the SOC to capture the shape of the curve at top of charge.

$$U = U^0 + \frac{RT}{F} \ln \left(\frac{\text{SOC}}{1 - \text{SOC}} \right) + \xi \cdot (\text{SOC}) + \alpha \cdot (\text{SOC})^2 + \beta \cdot (\text{SOC})^3 \quad (2)$$

Charge conduction— Charge conduction commonly occurs in batteries either by electrons moving through a conductive matrix or the movement of ions in an electrolyte. In the simplest form, the potential drop or inefficiencies from passing current may be related linearly to a resistance. These processes occur instantaneously and any time dependent behavior is related to parallel processes such as capacitance or the formation of concentration gradients. We delay discussion of concentration dependent conductivities to the section on mass transport. For a battery, a simple representation of both ionic and electronic voltage drops takes the form of Ohm's law, Eq (3).

$$\Delta V_c = IR_c \quad (3)$$

Here, ΔV_c is the voltage loss resulting from charge conduction of current, I , through resistance for charge conduction R_c . Batteries are composed of layers, and its energy/power content scale with area

rather than volume. Thus, it may be convenient to represent current and resistance terms in an area-specific manner. This is particularly true if one desires to scale up lab-scale testing to system level values. The modification of these equations to area-specific values is straightforward.

Charge transfer at an interface— Interfacial reactions are a defining characteristic of electrochemical energy storage and conversion devices as these reactions are where energy is stored or released within the electrodes. Non-faradaic reactions— where current flow is due to charge associated with movement of electrolyte ions, reorientation of solvent dipoles etc.—such as double layer capacitance, typically occur on time scales less than 1 s. We neglect these processes to focus on Faradaic reactions—where current flow is due to charge transferred during electrochemical reaction—which are of primary importance in batteries in contrast to capacitors. Charge transfer may take the form of an electron from a carbon electrode to a redox species in solution or an ion crossing the interface from an electrolyte into a host. Both of these processes are commonly described by a non-linear current voltage relationship. This relationship can be derived based on potential-modified activation energies for a reaction. The most common representation of this reaction is the Butler-Volmer equation shown in Eq (4) [32], a representation of the Butler-Volmer equation for the thermodynamics in Eq (1) evoking the common assumption of a transfer coefficient of 0.5. The interfacial current density i_j may be related to an electrode geometric area basis through multiplication by the specific interfacial area of the electrode. Here, k' is the combined rate parameter and V_j is the electrode potential.

$$i_j = nFk'_j \sqrt{C_{ox}C_{red}} \left\{ e^{0.5F/RT(V_j - U_j)} - e^{-0.5F/RT(V_j - U_j)} \right\} \quad (4)$$

Eq (4) is often linearized in the limit of facile kinetics. This has the benefit of removing the exponential terms and is often an adequate representation of a commercial system where the interface has been engineered to not be the limiting factor (i.e. not the rate determining step or largest source of overpotential). To capture the role of interfacial charge transfer at the battery level for both the negative and positive electrodes, we use Eq (5) as a linear representation of the summation of negative and positive charge transfer resistances based on Eq (4). Here, R'_k is a fitted parameter.

$$\Delta V_k = IR_k = \frac{IR'_k}{\sqrt{\text{SOC} \cdot (1 - \text{SOC})}} \quad (5)$$

Interfacial charge transfer occurs in parallel with capacitance at an electrified interface. The time constant associated with this resistance is commonly less than 1 s, but can become longer at high or low SOC as the resistance, R_k , increases. To maintain simplicity, we lump all time dependent phenomena under mass transport phenomena.

Mass transport— Concentration gradients typically form in the electrolyte or within the active materials during the passage of current. These gradients change the local concentration of the reactants at and/or through-out the electrode. Eq. (1) shows that a change in concentration will result in a change in OCV and thus cell voltage. This change in OCV appears to the operator of the battery as a voltage loss and thus caused by an apparent resistance. Concurrently, the average SOC of the battery is changing regardless of concentration gradients due to the finite capacity of the system. Thus, concentration gradients exaggerate the change in voltage that will be experienced if the current was interrupted and the system came to equilibrium at the average SOC in the battery.

A complicating factor is that the creation of concentration gradients is by its nature a time dependent phenomena that also depends on the magnitude of the current that is passed. The longer

the period of operation and greater magnitude of current in a single charge or discharge mode, the greater the concentration gradient that forms. Typically, a pseudo-steady-state condition is achieved at approximately three times the time constant for the process. Treatment of dilute solution or concentration solution based flux and material balance equations generally involves a numerical solution, but analytical solutions exist for a subset of circumstances. In an effort to obtain the 1st order time dependence, we use a hyperbolic tangent function that well-represents a time constant in an electrochemical system.

Using the derivative of Eq (2) for $dU/dSOC$, the apparent concentration resistance, R_U , may be defined by Eq (6) [33]. We treat this resistance as a time and SOC dependent function founded in the thermodynamics of the system. Here, dt is the time step in the simulation and Q is the rated Coulombic capacity of the battery. The second to last term in curly brackets in Eq (6) is the true thermodynamic change in the OCV of the system for the average SOC change [33]. The last term in curly brackets in Eq (6) is the influence of the concentration gradients on the apparent voltage of the battery. The last term ranges from unity at the limit of short durations to a fitted value R'_U at the limit of long durations. The onset of the apparent concentration resistance is related to a time constant τ fitted to experimental observations. The time t is the cumulative time spent operating the battery in a singular current direction, either charge or discharge.

$$\Delta V_U = IR_U = I \frac{dU}{dSOC} \cdot \frac{\Delta SOC}{I} = \frac{dU}{dSOC} \left\{ I \frac{dt}{Q} \left\{ 1 + \frac{R'_U}{2} \left[\left(1 + \tanh \left(\frac{2}{\tau} (t - \tau) \right) \right) \right] \right\} \right\} \quad (6)$$

Special cases for Eq (6) arise in the limit of short or long operation. Eq (7) holds for cases where the battery is operated using short pulses much less than the time constant, τ . Eq (8) holds for cases when the time step or cumulative time is much greater than τ , which can be further simplified to Eq. (9).

$$\Delta V_U = IR_U = I \frac{dU}{dSOC} \cdot \frac{\Delta SOC}{I} = \frac{dU}{dSOC} \left\{ IV_{ave} \frac{dt}{E} \right\} \text{ for } dt \text{ or } t \ll \tau \quad (7)$$

$$\Delta V_U = IR_U = I \frac{dU}{dSOC} \cdot \frac{\Delta SOC}{I} = \frac{dU}{dSOC} \left\{ IV_{ave} \frac{dt}{E} \right\} \{ 1 + R'_U \} \text{ for } dt \text{ or } t \gg \tau \quad (8)$$

$$\Delta V_U = IR_U = I \frac{dU}{dSOC} \cdot \frac{\Delta SOC}{I} = I \frac{dU}{dSOC} R'_{SOC} \quad (9)$$

2.1.1. Simplified non-linear EESS representation

The power of the battery, P_{batt} , is linked to the internal resistance and efficiency of the chemistry and battery design, as shown in Eq (10) [34]. The internal resistance, R , is the summation of the resistance contributions R_c , R_k , and R_U in Eqns (3), (5) and (6).

$$P_{batt} = U^2 \varepsilon_v (1 - \varepsilon_v) \varepsilon_{sys} / R \quad (10)$$

The generation or consumption of power is always coupled with losses. The electrochemical losses are represented by voltage efficiency, ε_v , and the system losses by the system efficiency, ε_{sys} . The battery losses can be rewritten explicitly as Eq. (10), where P_{tot} is the total power of the battery, without considering the voltage or system efficiency.

$$P_{loss} = P_{tot} (1 - \varepsilon_v \varepsilon_{sys}) = \frac{P_{batt}}{\varepsilon_v \varepsilon_{sys}} (1 - \varepsilon_v \varepsilon_{sys}) = U^2 (1 - \varepsilon_v) (1 - \varepsilon_v \varepsilon_{sys}) / R \quad (11)$$

Equation (10) may be rearranged to give the voltage efficiency as a function of battery power as in Eq (12). The voltage efficiency, ratio of battery voltage, V , to the open-circuit voltage, U , may be linearly related to the battery power if ε_v is close to unity as in Eq. (13). The linear approximation should be sufficiently accurate for $\varepsilon_v > 0.85$, which is the regime most grid storage batteries will operate.

$$\varepsilon_v = \frac{1}{2} + \sqrt{\frac{1}{4} - \frac{P_{batt} R}{U^2 \varepsilon_{sys}}} \quad (12)$$

$$\varepsilon_v \approx 1 - \frac{P_{batt} R}{U^2 \varepsilon_{sys}} \quad (13)$$

2.2. Scaling from cell to power plant

Assuming that a single cell type is used in the EESS, the performance of an individual cell may be scaled to represent the EESS performance at the level of a MW storage facility. The large-scale EESS is composed of many battery subunits connected in parallel. The battery subunits (i.e. packs) are typically composed of series connected cell groups. The cell groups will have individual cells connected in parallel. Other parallel-series configurations are possible, but are beyond the scope of this work and would have little impact on the calculated outcome. For brevity, we treat the parallel connected battery subunits at the level of cell groups. Appropriately summing the resistances in parallel and then series results in Eq (14). A complication left out of this work is the contact resistances formed by making the cell connections.

$$R = N_s R_{cell} / N_p \quad (14)$$

The number of cell groups in series, N_s , is the ratio of the battery voltage and the cell voltage. The number of cells in parallel, N_p , within a cell group is the battery capacity divided by the cell capacity. Substitution of these formulae into Eq (14) using the relationship between battery energy and capacity results in Eq (15).

$$R = \frac{U^o}{U^o_{cell}} R_{cell} \frac{Q_{cell}}{Q} = \frac{U^o}{U^o_{cell}} R_{cell} \frac{U^o Q_{cell}}{E} \quad (15)$$

Substituting Eq (15) in Eq (12) gives the SOC dependent Eq (16). Approximating battery OCV as the average OCV gives an SOC independent form of Eq (16) and resulting linear approximation in Eq (17), following the derivation of Eq (13).

$$\varepsilon_v = \frac{1}{2} + \sqrt{\frac{1}{4} - \frac{P_{batt}}{\varepsilon_{sys} E} \left[\frac{U^o}{U} \right]^2 \frac{R_{cell} Q_{cell}}{U^o_{cell}}} \quad (16)$$

$$\varepsilon_v \approx \frac{1}{2} + \sqrt{\frac{1}{4} - \frac{P_{batt}}{\varepsilon_{sys} E} \frac{R_{cell} Q_{cell}}{U^o_{cell}}} \approx 1 - \frac{P_{batt}}{\varepsilon_{sys} E} \frac{R_{cell} Q_{cell}}{U^o_{cell}} \quad (17)$$

Equations (16) and (17) give the voltage efficiency of the battery as a function of the total energy of the battery and the power used during operation. The last ratio on the right hand side in Eq (17) scales the losses to the measured performance of the physical cell. Using these two equations, Fig. 1a shows how the losses

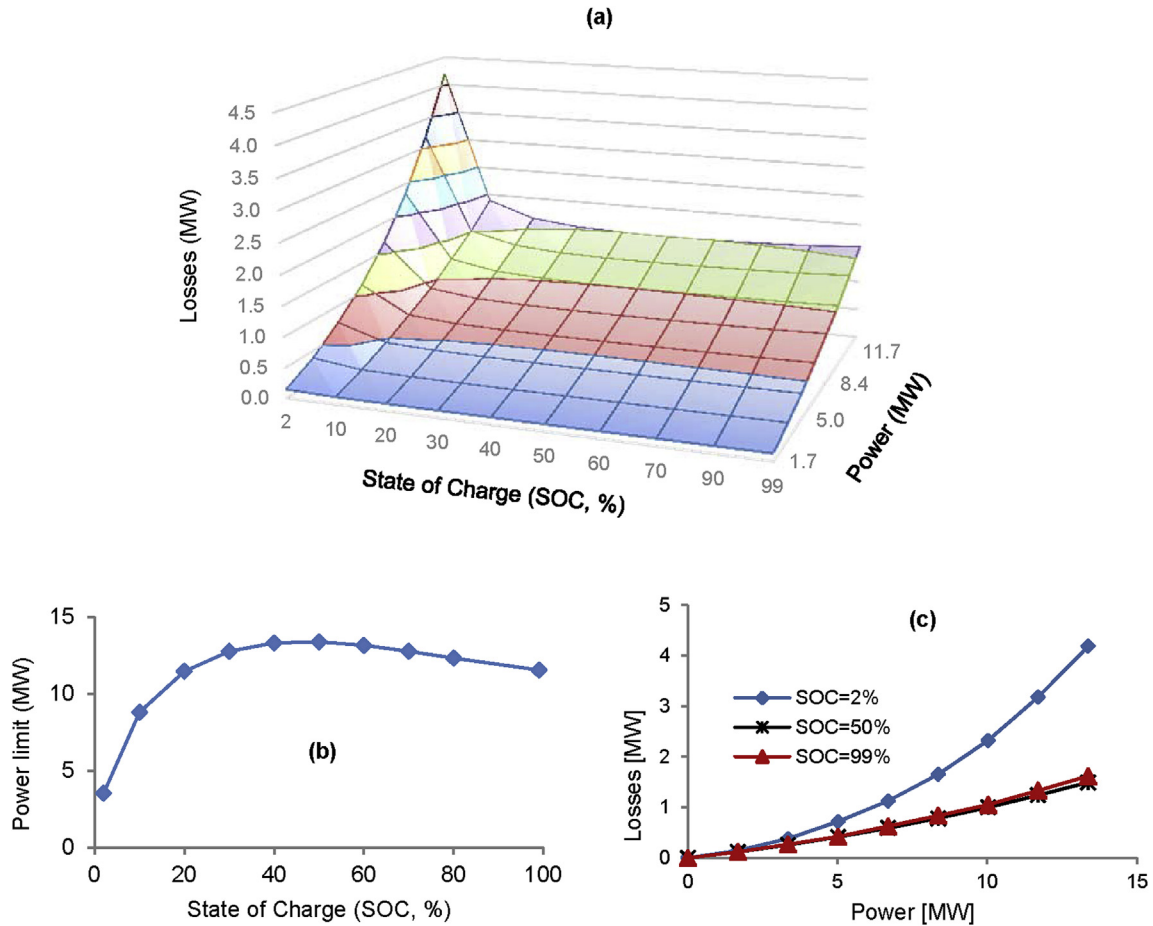


Fig. 1. Advanced representation of a 10 MWh li-ion battery pack using the proposed enhanced battery model showing (a) losses as function of power and SOC, (b) corresponding power limits for both charging and discharging as a function of SOC under the assumption of a 90% lower efficiency limit, and (c) corresponding losses as a function of the charge/discharge power at three different SOC levels.

depend on SOC and power levels for a 10 MWh battery. Higher losses are incurred at lower SOC levels, and higher power levels. Corresponding power limits as a function of the SOC that guarantees the operation of the battery at or above an assumed system efficiency limit of 90% are shown in Fig. 1b. Following the principle of microscopic reversibility [35], the same curve is used for both charging and discharging routines. System losses as a function of the discharge/charge power at three different states of charge has been shown in Fig. 1c. Piecewise linearized versions of the curves in Fig. 1b and c are implemented within the energy arbitrage model, as discussed in detail in Section 2.2.

2.2.1. Model validation

The parameters used to model the open circuit voltage (Equation (2)) were estimated using data from Sanyo's 2.05 A h LiNiCoMn cells discharged at a rate of C/5 (Fig. 2a). Performance data were obtained from the manufacturer's specification sheet, which were further verified previously in the laboratory using an Arbin BT2000 test stand [36]. The model was then used to predict the discharge curves for three other rates as shown in Fig. 2b–d. Delivered energies, both from the model as well as the manufacturers spec sheet were computed by calculating the area under the curves using the trapezoidal rule and the results were seen to be within 2.8% of one other.

2.3. A power systems energy arbitrage model with an improved linear representation of EESS

The basic energy arbitrage problem is a widely known problem by the power systems and energy storage communities and is therefore a suitable starting point to introduce more advanced battery representations, like the one proposed in this paper. For simplicity and clarity of exposition, we assume that the battery owner is a price taker with perfect ability to forecast prices. We consider historical real-time energy prices for one node (ALTW-FAIR.ST) in the MISO electricity market. The node is selected based on its high price volatility, which therefore makes it a priori a suitable location for energy storage investments. We focus the analysis on the real-time market, since day-ahead prices have much lower price volatility and present lower arbitrage opportunities. In sum, the perfect foresight assumption here represents an idealistic case that is likely to overestimate profit opportunities from energy arbitrage. On the other hand, we do not consider possible additional revenue streams, e.g. from provision of ancillary services, that would contribute to improve the profitability of EESS.

In this section, we first introduce the basic energy arbitrage model for energy storage with the simplest representation of EESS with fixed efficiency and power limits. Building on the simple model we introduce three additional models with more advanced battery representations, based on the proposed EESS representation. We also present the details of the linearized EESS

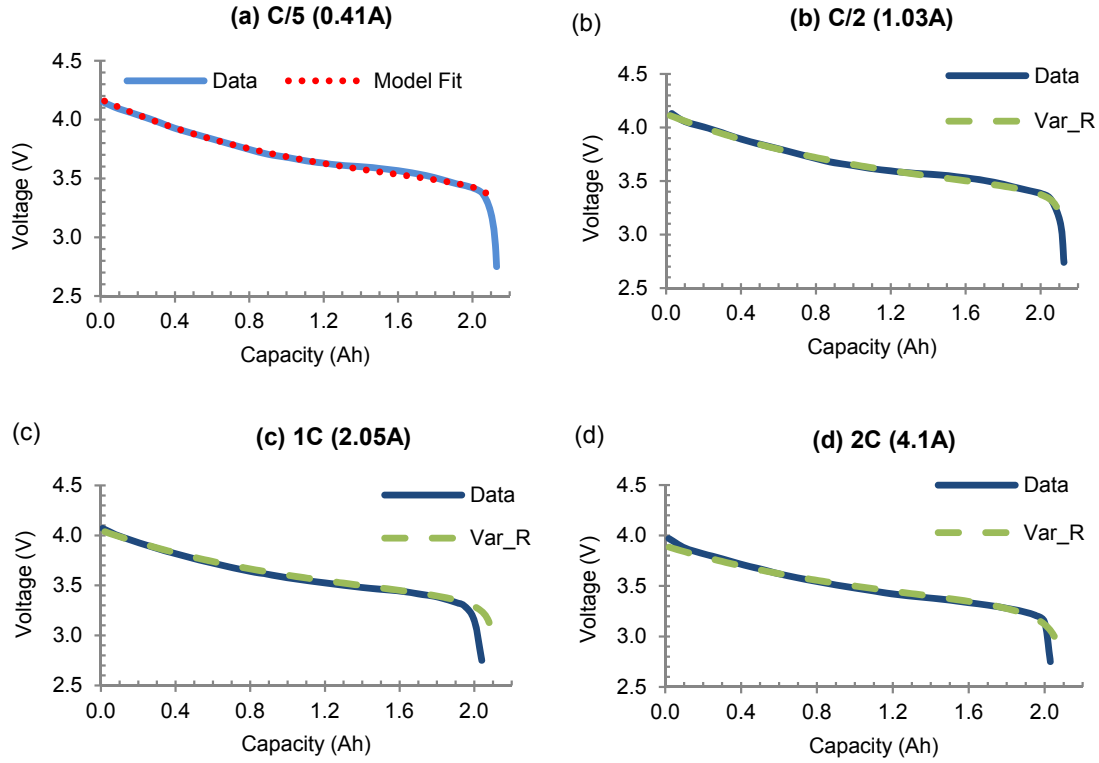


Fig. 2. Discharge data for a 2.05 Ah Sanyo LiNiCoMn spirally wound 18,650 cell from the manufacturer's specification sheet at a discharge rate of C/5 (0.41 A) was used to determine model parameters (a). The model (Var_R) was then tested for other discharge rates (b–d) and was found to accurately represent the data.

implementation within the arbitrage models and the assumptions used in the case study.

2.3.1. Arbitrage models

A widely known use of energy storage in the power grid is to buy/sell electricity from/to the power grid. The idea is that the storage owner can buy and store electricity when the prices are low and sell it back to the grid when the prices are high, thereby making a profit through so-called energy arbitrage. Here we focus on the arbitrage profit maximization of a battery storage owner, a problem which is widely studied in the literature [9,37,38]. A basic energy arbitrage maximization problem, M0, is given by the mathematical program that uses Eqs. (18)–(28):

$$(M0) \quad \max \sum_{t=1}^T p^{RT}(t) [E^S(t) - E^P(t)] \quad (18)$$

Subject to:

$$E^P(t) = P_c(t)\gamma(1 + \eta) \quad \forall t \quad (19)$$

$$E^S(t) = P_d(t)\gamma/(1 + \eta) \quad \forall t \quad (20)$$

$$P_c(t) \leq P_c^{max}w(t) \quad \forall t \quad (21)$$

$$P_d(t) \leq P_d^{max}(1 - w(t)) \quad \forall t \quad (22)$$

$$C(1) = C^0 - \gamma P_d(1) + \gamma P_c(1) \quad (23)$$

$$C(t) = C(t-1) - \gamma P_d(t) + \gamma P_c(t) \quad \forall t \geq 2 \quad (24)$$

$$C^{min} \leq C(t) \leq C^{max} \quad \forall t \quad (25)$$

$$(1 - \lambda)C^0 \leq C(T) \leq (1 + \lambda)C^0 \quad (26)$$

$$E^S(t), E^P(t), P_c(t), P_d(t), C(t) \geq 0 \quad \forall t \quad (27)$$

$$w(t) \in \{0, 1\} \quad \forall t \quad (28)$$

The objective function in M0 is to maximize arbitrage profits, i.e., revenue from sales minus cost of purchases given the real-time electricity price. Constraints shown in Eqs. (19) and (20) reflect the efficiency losses for charging and discharging at a given time step; the time step coefficient, γ , takes the value of 1/12 for 5-min resolution and 1 for 60-min resolution. Efficiency loss is represented as a constant with parameter η . Eqs. (21) and (22) ensure that the battery's charging rate is lower than its limits while also ensuring that it does not charge and discharge at the same time, where the binary variable $w(t)$ is set to 1 when it is charging and 0 otherwise. The binary charge/discharge variable is necessary to avoid charging and discharging to take place at the same time during negative prices, which may occur in electricity markets. The battery's energy level, or SOC, is updated by Eqs. (23) and (24). The battery's energy limits are taken into account in (25). Eq. (26) ensures that battery's energy level at the end of the optimization horizon is within a tolerance of its initial condition. Finally, Eqs. (27) and (28) impose the non-negativity on the continuous variables and define the binary variable for charge/discharge.

In the basic arbitrage maximization model, power limits and

efficiency losses are constants. Next, building on the basic model, M0, we develop models that take into account variable power limits and efficiency losses using the EESS representation derived in section 2.1. We consider three variations:

- M1: charge/discharge power limits as a function of SOC
- M2: charge/discharge efficiency losses as a function of power charged/discharged
- M3: charge/discharge power limits as a function of SOC and charge/discharge efficiency losses as a function of power charged/discharged and SOC

First, in model M1 we model the maximum charging and discharging limits as functions of the SOC. Note that, in M0, the maximum charging/discharging rates, P_c^{max} and P_d^{max} are constants in Eqs. (21) and (22). As discussed in Section 2.1.1, in reality the relationship between the maximum charging (discharging) rates and the SOC is non-linear. We use step-wise linear functions, as illustrated in Fig. 1b, to model the nonlinear battery relationships described in section 2.1. We formulate M1 as follows:

$$(M1) \quad \max \sum_{t=1}^T p^{RT}(t) [E^S(t) - E^P(t)]$$

Subject to: Eqs. (19)–(28)

$$\beta(1) = [C^0 + C(1)] / [2 \cdot C^{max}] \quad (29)$$

$$\beta(t) = [C(t-1) + C(t)] / [2 \cdot C^{max}] \quad \forall t \geq 2 \quad (30)$$

$$\sum_{j=1}^J y(t,j) s_c(j) = \alpha_c(t) \quad \forall t \quad (31)$$

$$\sum_{j=1}^J y(t,j) = \beta(t) \quad \forall t \quad (32)$$

$$y(t,j) \leq b(j) z_c(t,j) \quad \forall t, j \quad (33)$$

$$y(t, j-1) \geq b(j-1) z_c(t,j) \quad \forall t, j \geq 2 \quad (34)$$

$$\sum_{i=1}^I x(t,i) s_d(i) = \alpha_d(t) \quad \forall t \quad (35)$$

$$\sum_{i=1}^I x(t,i) = \beta(t) \quad \forall t \quad (36)$$

$$x(t,i) \leq a(i) z_d(t,i) \quad \forall t, i \quad (37)$$

$$x(t, i-1) \geq a(i-1) z_d(t,i) \quad \forall t, i \geq 2 \quad (38)$$

$$P_c(t) \leq P_c^{max} \cdot \alpha_c(t) \quad \forall t \quad (39)$$

$$P_d(t) \leq P_d^{max} \cdot \alpha_d(t) \quad \forall t \quad (40)$$

$$\alpha_c(t), \alpha_d(t), \beta(t) \geq 0 \quad \forall t \quad (41)$$

$$x(t,i), y(t,j) \geq 0 \quad \forall t, i, j \quad (42)$$

$$z_c(t,j), z_d(t,i) \in \{0, 1\} \quad \forall t, i, j \quad (43)$$

In M1, $\beta(t)$ is the fraction of the battery that is charged in period t . It is defined as the average fraction in the current period and the previous period by Eqs. (29) and (30). We define $\alpha_c(t)$ and $\alpha_d(t)$ as the variables representing the fractions of the maximum battery limits that are usable in period t for charge and discharge respectively. Eqs. (31)–(38) set up the piece-wise linear functions for charging and discharging respectively. The non-linear curve is partitioned into J pieces for charging and I pieces for discharging. Eqs. (31) and (35) compute the fractions of charging and discharging limits available given the components of SOC level and linearized slopes of the relationship between SOC and fraction of power rate available. Eqs. (32) and (36) make sure that the SOC components of the piece-wise linear function sum up to the SOC level in period t . The pieces of the piece-wise linear functions for SOC level are defined by parameters $b(j)$ and $a(i)$ for charging and discharging, respectively. Eqs. (33) and (37) ensure that the SOC components of the piece-wise linear functions are less than or equal to $b(j)$ for charging and $a(i)$ for discharging if the piece is active, i.e., $z_c(t,j)$ is 1 for charging, $z_d(t,i)$ is 1 for discharging. We also make sure that if a later piece is active, the piece before it must be active by the constraints represented by Eqs. (34) and (38). Eqs. (39) and (40) limits the maximum charging/discharging limits given the fractions $\alpha_c(t)$ and $\alpha_d(t)$. Note that if the battery is charging, (39) dominates (21) and if the battery is discharging (40) dominates (22). Eqs. (41)–(43) ensure non-negativity and set up the binary variables.

Next, also building on the basic model M0, we introduce charge/discharge efficiency losses as a function of charge/discharge level in model M2.

$$(M2) \quad \max \sum_{t=1}^T p^{RT}(t) [E^S(t) - E^P(t)]$$

Subject to: Eqs. (21)–(28)

$$E^P(t) = \gamma [P_c(t) + P_c^{loss}(t)] \quad \forall t \quad (44)$$

$$E^S(t) = \gamma [P_d(t) - P_d^{loss}(t)] \quad \forall t \quad (45)$$

$$\sum_{l=1}^L v_c(t,l) s_c^{loss}(l) = P_c^{loss}(t) \quad \forall t \quad (46)$$

$$\sum_{l=1}^L v_c(t,l) = P_c(t) \quad \forall t \quad (47)$$

$$v_c(t,l) \leq d(l) z_c^{loss}(t,l) \quad \forall t, l \quad (48)$$

$$v_c(t, l-1) \geq d(l-1) z_c^{loss}(t,l) \quad \forall t, l \geq 2 \quad (49)$$

$$\sum_{l=1}^L v_d(t,l) s_d^{loss}(l) = P_d^{loss}(t) \quad \forall t \quad (50)$$

$$\sum_{l=1}^L v_d(t,l) = P_d(t) \quad \forall t \quad (51)$$

$$v_d(t, l) \leq c(l)z_d^{\text{loss}}(t, l) \quad \forall t, l \quad (52)$$

$$v_d(t, l-1) \geq c(l-1)z_d^{\text{loss}}(t, l) \quad \forall t, l \geq 2 \quad (53)$$

$$P_c^{\text{loss}}(t) \leq P_c^{\text{max}}w(t) \quad \forall t \quad (54)$$

$$P_d^{\text{loss}}(t) \leq P_d^{\text{max}}(1-w(t)) \quad \forall t \quad (55)$$

$$P_c^{\text{loss}}(t), P_d^{\text{loss}}(t) \geq 0 \quad \forall t \quad (56)$$

$$v_c(t, l) \geq 0 \quad \forall t, l \quad (57)$$

$$v_d(t, l) \geq 0 \quad \forall t, l \quad (58)$$

$$z_c^{\text{loss}}(t, l) \in \{0, 1\} \quad \forall t, l \quad (59)$$

$$z_d^{\text{loss}}(t, l) \in \{0, 1\} \quad \forall t, l \quad (60)$$

In M2, constraints represented by Eqs. (19) and (20) are replaced by Eqs. (44) and (45) to account for the variability of efficiency losses: instead of using the efficiency loss parameter, η , the losses are computed now as a function of charge and discharge levels. The linear step-wise functions for charge/discharge level and losses in M2 are set up similarly to the SOC and fraction of power limits relationship in M1. We assume that the same number of pieces, L , are selected both for charging and discharging. The computed power charge loss is added to the charge level in Eq. (44) and power discharge loss is subtracted from the discharge level in Eq. (45). Losses cannot be greater than the maximum charging and discharging limits by Eqs. (54) and (55). Eqs. (56)–(60) ensure non-negativity and set up the binary variables for the piecewise loss functions.

Finally, in model M3, which is the most advanced battery representation, we model charge/discharge efficiency losses as a function of both charge/discharge level and SOC. To formulate this, we define a partition on SOC percentage of the battery as follows:

$$\{0 = B(1) < B(2) \dots < B(K) = 1\}$$

We denote the activation function with $u = \{u(t, k), k = 1, \dots, K\}$ where K is the number of curves. There exists a non-linear curve for every SOC level. The activation function is defined as:

$$u(t, k) = \begin{cases} 1 & \text{if } \beta(t) \in [B(k), B(k+1)] \\ 0 & \text{if } \beta(t) \notin [B(k), B(k+1)] \end{cases}$$

Model M3 also considers that power limits are a function of SOC, using the same implementation as in model M1. Let M be a big number. Then model M3 is formulated as:

$$(M3) \quad \max \sum_{t=1}^T p^{\text{DA}}(t) [E^{\text{S}}(t) - E^{\text{P}}(t)]$$

Subject to: Eqs. (21)–(45), (47)–(49), (51)–(60)

$$\sum_{k=1}^K u(t, k) = 1 \quad \forall t \quad (61)$$

$$\beta(t) \leq \sum_{k=1}^K u(t, k) \cdot B(k+1) \quad \forall t \quad (62)$$

$$\beta(t) \geq \sum_{k=1}^K u(t, k) \cdot B(k) \quad \forall t \quad (63)$$

$$P_c^{\text{loss}}(t) \leq \sum_{l=1}^L v_c(t, l) s_c^{\text{loss}}(l, k) + M(1 - u(t, k)) \quad \forall t, k \quad (64)$$

$$P_c^{\text{loss}}(t) \geq \sum_{l=1}^L v_c(t, l) s_c^{\text{loss}}(l, k) - M(1 - u(t, k)) \quad \forall t, k \quad (65)$$

$$P_d^{\text{loss}}(t) \leq \sum_{l=1}^L v_d(t, l) s_d^{\text{loss}}(l, k) + M(1 - u(t, k)) \quad \forall t, k \quad (66)$$

$$P_d^{\text{loss}}(t) \geq \sum_{l=1}^L v_d(t, l) s_d^{\text{loss}}(l, k) - M(1 - u(t, k)) \quad \forall t, k \quad (67)$$

$$u(t, k) \in \{0, 1\} \quad \forall t, k \quad (68)$$

In M3, we replace constraints represented by Eqs. (46) and (50) in M2 by Eqs. (61)–(68). The added constraints compute the power losses as a function of charge/discharge levels as well as predefined K number of SOC levels. Through the constraint represented by Eq. (61), only one SOC level can be active in a given time period t . Eqs. (62) and (63) make sure that the SOC level in period t , $\beta(t)$, is less than or equal to the active SOC level for which $u(t, k)$ is 1 and greater than or equal to the previous SOC level. Eqs. (64)–(67) ensure that the slopes for the active SOC level are used to compute the power loss for charging and discharging. Eq. (68) defines the binary activation function for SOC levels.

2.3.2. Linearized EESS representation in arbitrage model

The implementation of power limits and losses with piecewise linear representations is illustrated in Fig. 3 for all advanced models considered in the case study presented in the next section.

Fig. 3a presents the relationship between SOC and power limits, which are applied in models M1 and M3. The same curve is used for both charging and discharging. The linearization of the non-linear curve is achieved through the step-wise linearization, as illustrated in the figure. The maximum power limits occur for the middle SOC range.

Fig. 3b shows the relationship between power and losses, which is applied in model M2. The same curve is used both for charging and discharging. As power input/output of the battery increases the losses are greater. The marginal losses are also increasing with higher power limits. The curve in Fig. 3b is estimated from the battery model based on a SOC-level of 50%, as the model M2 does not consider the impact of SOC on losses. In contrast, Fig. 3c shows the power and losses relationship for different SOC levels that apply to model M3. The relationship between losses and SOC are nonlinear, but linearized through step-wise functions using five curves for different SOC levels, all with constant power segments. Losses are greatest when the battery is empty and the lowest when it is half way full.

2.3.3. Assumptions and parameters

We use real-time prices from the ALTW.FAIR_ST node in the MISO market for the week of August 19–25 2013 (prices were

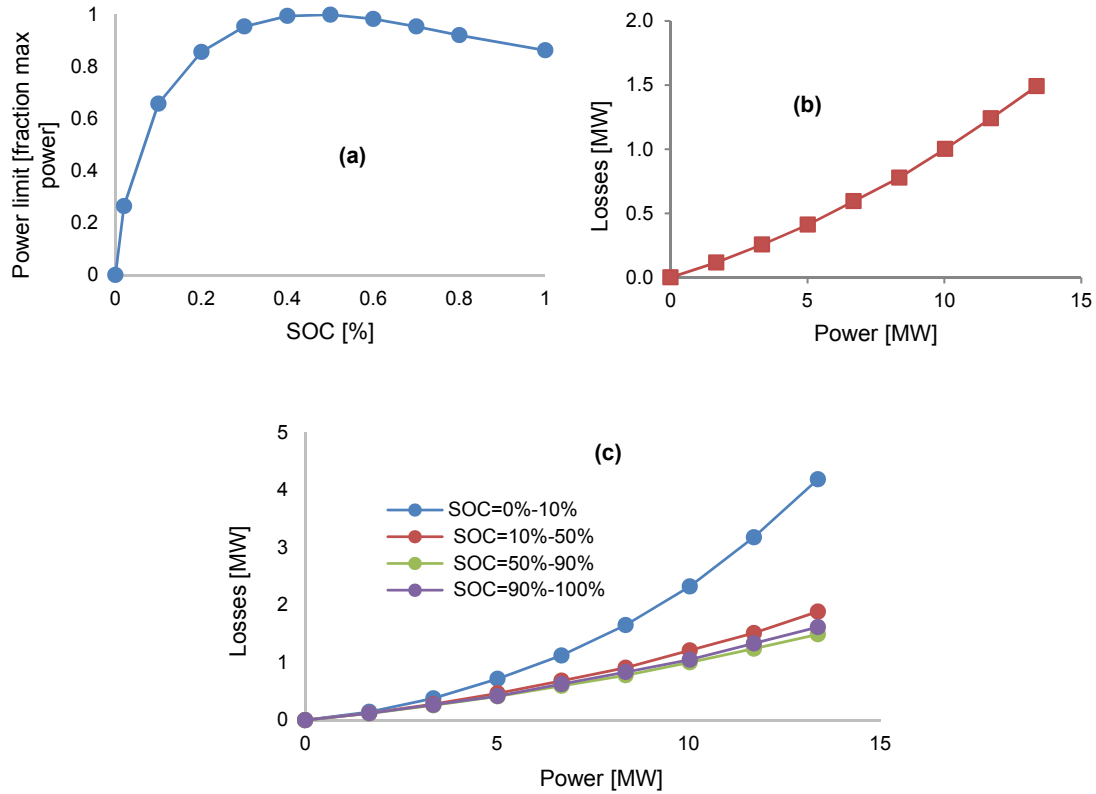


Fig. 3. Linearized implementation of (a) power limits as a function of SOC (b) losses as a function of power (c) losses as a function of power and SOC within arbitrage model.

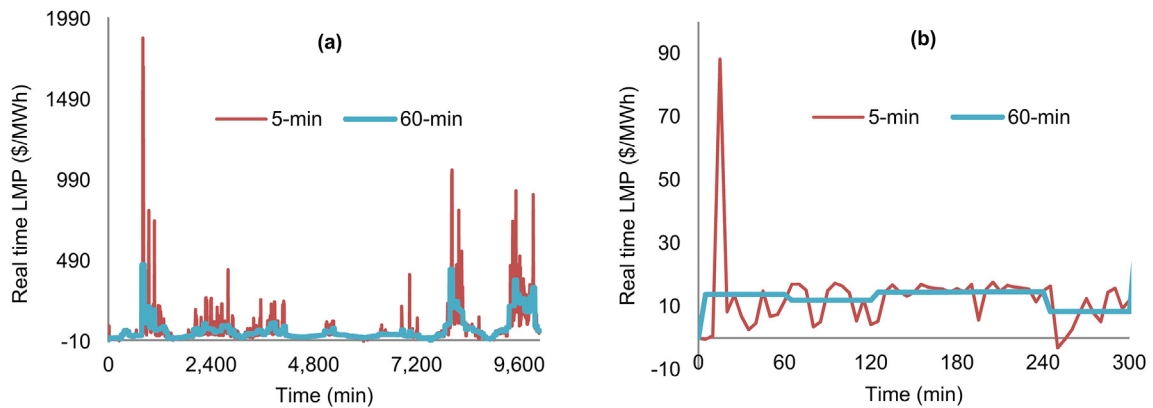


Fig. 4. Hourly and 5min energy prices in the ALTW.FAIR_ST node in the MISO market for periods (a) Aug 19–25 and (b) Aug 19, hour 1–5.

accessed from MISO’s website). This node was selected as it exhibits large price volatility and therefore is a good candidate for energy arbitrage applications. The selected week represents peak load conditions with high prices and also high volatility in prices. In our analysis, we use both 5 min and hourly time resolution of prices (shown in Fig. 4) given that with the recent FERC ruling MISO will change from hourly to 5 min prices for financial settlement soon.² We investigate the possible implications for energy storage profits of this change in market rules during the one-week period used in the analysis. The boundary conditions at the end of the period are

² Note that 5 min prices were already calculated in 2013, but not used for financial settlements.

established through a wrap-up tolerance, i.e., battery’s energy level at the end of the optimization horizon is within a tolerance of its initial condition. The basic parameters used in the models are given in Table 1.

3. Results and discussion

The objective of this work is to test the effects of an enhanced representation of lithium-ion batteries in an energy arbitrage model designed to maximize profits under different resolution price signals. Electricity price data at both 5- and 60-min resolutions were used for this purpose. For the base-case model MO—fixed power limit and fixed efficiency—, the weekly profits obtained by the lithium-ion battery system using price data with 5-

Table 1
Battery parameters that are used in the numerical study.

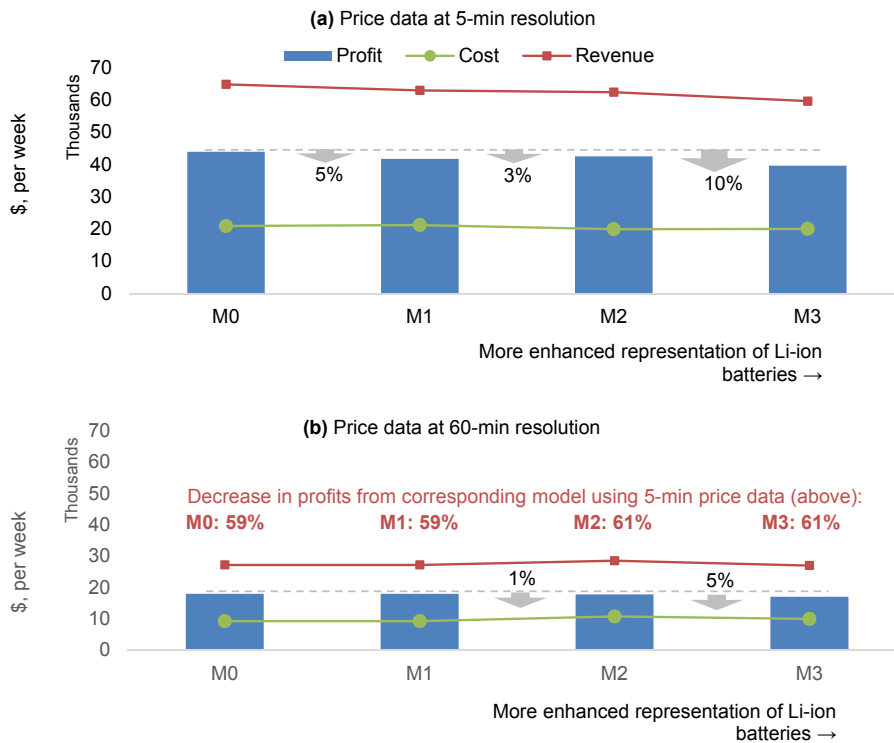
Parameter	Value	Unit
η	10	%
C^0	5	MWh
C^{max}	10	MWh
C^{min}	0.1	MWh
p_c^{max}	13.37	MW
p_d^{max}	13.37	MW
λ	1	%
γ	1/12 or 1	hour

min resolution were \$43.9 k, which dropped by 59% to \$17.9 k using price data with 60-min resolution (Fig. 5 and Table 2). As the battery models were gradually enhanced from M0 to M3—and consequently gradually constrained by the physical limitations of the battery—we see a drop in weekly profits from \$43.9 k for M0 to \$39.6 k for M3—a 10% drop— when price data with a 5-min resolution is used. The M1 model—where only the power limits are expressed as a function of the SOC— estimated a 5% decrease in profit, while the M2 model— in which the efficiency is expressed as a function of the charging and discharging power— produced a 3% decrease. When price data with a 60-min resolution was used (Fig. 5b), the estimated profits decreased by 5% with the battery model enhancements from \$17.9 k for M0 to \$17 k for M3.

Introducing SOC-dependent power limits in the battery model (M1) did not impact profits in the 60-min. resolution analysis; while making the efficiency dependent on the power charge/discharge in model M2 decreased profits by only 1% compared to the M0 case. These profits along with the revenues and costs have been summarized in Table 2.

The observed decrease in profits when a 60-min price signal is used vs. a 5-min signal comes as no surprise when the variation in these price signals is compared (Fig. 4). The more volatile nature of the 5-min price profile guarantees more opportunities for arbitrage than the 60-min profile (Fig. 4b). Fig. 6 shows the time-variation of the SOC, charging and discharging losses, and the charging and discharging power across the different models for both the 5-min and the 60-min resolution price data. These values are useful in order to further understand the calculated profits.

Fig. 6a and b shows that the variation of the SOC of the 10 MWh lithium-ion battery used in this study during the first five hours of the modeling timeframe. As expected, the plot showing the variation with a 5-min resolution price signal (Fig. 6a) shows a larger variability compared to the 60-min one (Fig. 6b). This is also true for the losses and the charging and discharging powers (Fig. 6c–h). It is seen that with increasing model enhancements the SOC operating window shrinks due to the more realistic variation of the power limits and the operating losses. The underestimation of losses with a fixed power-limit and efficiency in the case of model M0 compared to when they are represented more realistically, as in the



Model description: **M0:** Fixed power limits, fixed efficiency; **M1:** SOC dependent power limits, fixed efficiency; **M2:** Fixed power limits, efficiency as a function of power; **M3:** SOC dependent power limits, efficiency as a function of power and SOC.

Fig. 5. Effects of an enhanced representation of lithium-ion batteries in an energy arbitrage model designed to maximize profits with a) price data at 5-min resolution and b) price data at 60-min resolution. Profits are seen to be lower by up to 61% for price data with 60-min resolution, while the variation across the models (M0–M3) with increasingly enhanced representation of lithium-ion batteries are less pronounced. For price data at 5-min resolution, a simple representation with fixed power limits and efficiency (M0) results in a 10% overestimation of profits compared to when the power limit is varied as a function of the SOC (M1) and the efficiency is varied as a function of the SOC and the charge and discharge power (M3). Varying only the power as a function of the SOC (M1) shows a 5% decrease in profits while varying only the efficiency shows a slightly higher decrease in the estimated profits at 3%. These differences are less pronounced when the price data is at a 60-min resolution with only a 5% drop in profits between M0 and M3.

Table 2

Summary of revenue, cost and profit numbers from the arbitrage model for the different models with increasingly enhanced representation of lithium-ion batteries.

	M0		M1		M2		M3	
	5-min	60-min	5-min	60-min	5-min	60-min	5-min	60-min
Revenue	64,753	27,153	62,872	27,153	62,323	28,484	59,549	26,950
Cost	20,882	9216	21,187	9216	19,895	10,736	19,997	9933
Profit	43,872	17,937	41,685	17,937	42,428	17,748	39,552	17,017

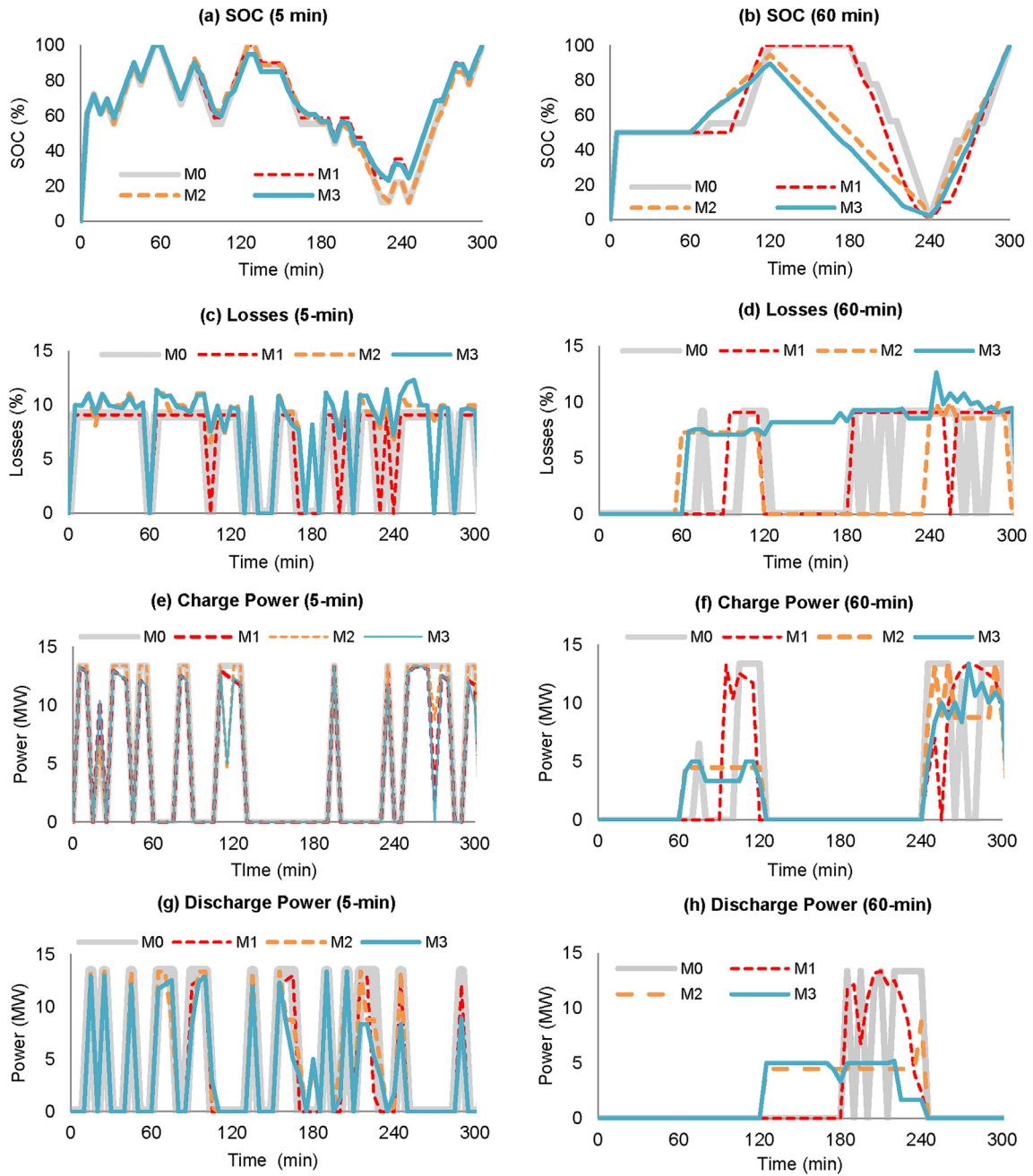


Fig. 6. State of charge (a–b), losses (c–d), charge (e–f) and discharge (g–h) power variation over a period of 5 h. With higher, 5-min resolution price data, the curves are seen to be noisier as expected. The operating SOC window is seen to be narrower for M3 compared to M0 likely as a result of the variable power limits (a–b). Losses are also seen to be higher and more variable for M2 and M3 compared to M0 and M1 (c–d). Charge and discharge at higher power levels also decreases from M0 to M3 (e–h).

case of model M3, is clear from Fig. 6c and d. Charge and discharge power levels are also lower for M3 compared to M0. These performance characteristics of the battery, resulting from the battery

model enhancements, lead to a more accurate estimation of the arbitrage profits.

Enhanced representations, however, come at the cost of higher

Table 3
Computational effort to solve the different models.

Model	Price Signal	Time (s)
M0	5 Min	2.6
	60 Min	3.4
M1	5 Min	809.2
	60 Min	100
M2	5 Min	46.9
	60 Min	48.2
M3	5 Min	268,497.3
	60 Min	780,863.8

computational times. The time to solve the models M0–M3 have been compared in Table 3. The values reported are for one processing core calculated by multiplying the number of cores used and the solution time. Not surprisingly, we see that the base case model M0 has the fastest solution time given the simple representation of the lithium-ion batteries in it, averaging about 3 s for both the 5-min and the 60-min price signals. On the other side of the spectrum, model M3 takes 74.5 h and 217 h for the 5- and 60-min price signals, respectively—substantially longer than model M0. In the case of M1, we see that the 5-min price signal takes longer to solve, which could simply be resulting from the higher resolution price data compared to the 60-min signal. In the case of M3, however, it takes significantly longer to solve with the 60-min price signal—comprised of twelve data points of the same price at 5-min intervals. The reason may be that multiple identical price points several optimal solutions may exist and this does not help the model converge any faster. Model M2, in which the power limits remain fixed but the efficiency is varied as a function of the charge and discharge powers, stands out as the enhancement with the lowest computational cost with solution times of less than 50 s.

4. Summary and conclusions

We develop novel enhanced representations of the physical phenomena in of lithium-ion batteries and investigate the effects of these new representations on the profits obtained by an electrochemical energy storage system in an energy arbitrage model. We also examine the effect of a 5-min price signal vs. a 60-min one on the battery's profitability. The proposed representations can serve as a generic framework that captures the physical phenomena characterizing the behavior of EESSs into a mixed-integer-linear formulation. This generic formulation can be directly implemented in a range of different power systems models. We test the applicability of the proposed EESS formulation within an energy arbitrage model that maximizes the profits from a lithium-ion battery pack that buys and sells energy from the grid, using price data from the MISO market.

We find that when the power-limits and efficiency of a battery are more accurately represented, profits from the arbitrage model decreased by as much as 10% compared to when these performance characteristics of the battery are held constant. However, the most enhanced model, M3, took substantially longer time to produce a solution compared to the basic model, M0. An intermediate model, M2, in which only the efficiency was represented more accurately performed much better in terms of computational time. Results from this study also show that increasing the time resolution of the price signal, from 60- to 5-mins, resulted in a 60% increase of profits from arbitrage maximization.

4.1. Future work

An important feature of the proposed battery model is that it

can be incorporated into any power systems optimization model formulated as a MILP problem. In future work, we plan to test the battery model on other applications in the power system, including system-wide unit commitment, economic dispatch, and generation/transmission planning. We will also use the proposed battery model, which is generic in nature, on different battery chemistries beyond Li-ion batteries.

An important limitation of the analysis is that the battery model currently does not account for the degradation associated with lithium-ion batteries, which is likely going to have a substantial impact on the profitability of the system. The thermal management of the battery system is expected to impact degradation along with the system's efficiency. Improved understanding of thermal management together with degradation and its effect on battery lifetime, profitability, and optimal operational are important directions for future work.

Nomenclature

Battery model

Chemistry agnostic variables/constants

E	Battery energy
P_{batt}	Battery power
U^0	Battery OCV at 50% SOC (Nominal battery voltage)
Q	Battery nominal capacity, $E/U^0 = Q$
a_{ox}	Activity of the oxidant
a_{red}	Activity of the reductant
R	Gas constant, 8.314 J/mol.K
T	Temperature
n	number of moles of electrons transferred in the balanced equation for the reaction occurring in the cell
F	Faraday's constant (96,485 C/mole)

Chemistry specific parameters (Fitted)

ξ	Empirical first order parameter to modify slope of battery OCV vs SOC function, V
α	Empirical second order parameter to modify slope of battery OCV vs SOC function, V
β	Empirical third order parameter to modify slope of battery OCV vs SOC function, V
R_c	Resistance to charge conduction or high frequency resistance, Ohm
R'_k	Kinetic resistance scaling factor, Ohm
R'_{SOC}	Empirical state-of-charge based resistance scaling factor, Ohm V^{-1}
R'_U	Thermodynamic resistance scaling factor, Ohm
τ	Time constant for mass transport, sec
ε_{sys}	System efficiency not including electrochemical losses

Optimization

Indices

t	time periods, $t = 1, \dots, T$
i	pieces of the piece-wise linear function for discharge limit, $i = 1, \dots, I$
j	pieces of the piece-wise linear function for charge limit, $j = 1, \dots, J$
m	pieces of the piece-wise linear function for charge/discharge loss, $m = 1, \dots, M$
k	SOC percentage level of efficiency loss curve for charge/discharge state, $k = 1, \dots, K$

Parameters

$p^{RT}(t)$	real-time (RT) electricity price in period t
-------------	--

η	losses (one-way)
C^0	initial state of charge
C^{max}, C^{min}	maximum and minimum state of charge
P_c^{max}	maximum charge rate
P_d^{max}	maximum discharge rate
λ	wrap-up tolerance
γ	time step coefficient
$s_d(i)$	slope of piece i for discharge limit piece-wise linear function
$a(i)$	size of piece i
$s_c(j)$	slope of piece j for charge limit piece-wise linear function
$b(j)$	size of piece j
$s_d^{loss}(m)$	slope of piece m for discharge loss piece-wise linear function (M2)
$s_d^{loss}(m, k)$	slope of piece m for discharge loss piece-wise linear function for SOC level k (M3)
$c(m)$	size of piece m
$s_c^{loss}(m)$	slope of piece m for charge loss piece-wise linear function (M2)
$s_c^{loss}(m, k)$	slope of piece m for charge loss piece-wise linear function for SOC level k (M3)
$d(m)$	size of piece m
$B(k)$	partition on SOC percentage, $k = 1, 2, \dots, K$

Decision variables

$E^S(t)$	energy sold to RT market in period t (discharge)
$E^P(t)$	energy purchased from RT market in period t (charge)
$P_c(t)$	power charged in period t
$P_d(t)$	power discharged in period t
$C(t)$	state of charge in period t
$\alpha_c(t)$	fraction of maximum charge rate that could be used in period t
$\alpha_d(t)$	fraction of discharge rate that could be used in period t
$\beta(t)$	fraction of battery that is used in period t
$x(t, i)$	fraction of battery used in period t for piece i
$y(t, j)$	fraction of battery used in period t for piece j
$z_d(t, i)$	1 if piece i is active in period t , 0 otherwise
$z_c(t, j)$	1 if piece j is active in period t , 0 otherwise
$w(t)$	1 if battery is charging in period t , 0 otherwise
$P_c^{loss}(t)$	charge loss in period t
$P_d^{loss}(t)$	discharge loss in period t
$v_d(t, m)$	discharge amount for piece m in period t
$z_d^{loss}(t, m)$	1 if piece m is active in period t , 0 otherwise
$v_c(t, m)$	charge amount for piece m in period t
$z_c^{loss}(t, m)$	1 if piece m is active in period t , 0 otherwise
$u(t, k)$	activation function for state of charge level k in period t

References

- [1] A.A. Akhil, et al., DOE/EPRI 2013 Electricity Storage Handbook in Collaboration with NRECA, Report SAND2013-5131, Sandia National Laboratory, 2013.
- [2] U.S. Department of Energy, DOE Global Energy Storage Database, 2012. <http://www.energystorageexchange.org/> (Accessed 30 August 16).
- [3] H. Su, A.E. Gamal, Modeling and analysis of the role of energy storage for renewable integration: power balancing, *IEEE Trans. Power Syst.* 28 (4) (2013) 4109–4117.
- [4] N. Li, K. Hedman, Economic assessment of energy storage in systems with high levels of renewable resources, *IEEE Trans. Sustain. Energy* 6 (3) (2015) 1103–1111.
- [5] N. Li, C. Uckun, E. Constantinescu, J.R. Birge, K.W. Hedman, A. Botterud, Flexible operation of batteries in power system scheduling with renewable energy, *IEEE Trans. Sustain. Energy* 7 (2) (2016) 685–696.
- [6] D. Pudjianto, M. Aunedi, P. Djapic, G. Strbac, Whole-systems assessment of the value of energy storage in low-carbon electricity systems, *IEEE Trans. Smart Grid* 5 (2) (2014) 1098–1109.
- [7] F. de Sisternes, J. Jenkins, A. Botterud, The value of energy storage in decarbonizing the electricity sector, *Appl. Energy* 175 (2016) 368–379.
- [8] R. Sioshansi, P. Denholm, T. Jenkins, J. Weiss, Estimating the value of electricity storage in PJM: arbitrage and some welfare effects, *Energy Econ.* 31 (2) (2009) 269–277.
- [9] K. Bradbury, L. Pratsun, D. Patiño-Echeverri, Economic viability of energy storage systems based on price arbitrage potential in real-time U.S. electricity markets, *Appl. Energy* 114 (2014) 512–519.
- [10] H. Mohsenian-Rad, Optimal bidding, scheduling, and deployment of battery systems in California day-ahead energy market, *IEEE Trans. Power Syst.* 31 (1) (2016).
- [11] R.H. Byrne, C.A. Silva-Monroy, Estimating the Maximum Potential Revenue for Grid Connected Electricity Storage: Arbitrage and Regulation, Sandia 2012-3863, Sandia National Laboratory, 2012.
- [12] D. McConnell, T. Forcey, M. Sandiford, Estimating the value of electricity storage in an energy-only wholesale market, *Appl. Energy* 159 (2015) 422–432.
- [13] P. Denholm, M. Hand, Grid flexibility and storage required to achieve very high penetration of variable renewable electricity, *Energy Policy* 39 (3) (2011) 1817–1830.
- [14] International Energy Agency, The Power of Transformation—wind, Sun and the Economics of Flexible Power Generation, Available at: https://www.iea.org/publications/freepublications/publication/The_power_of_Transformation.pdf (Accessed 30 August 16).
- [15] A. Sakti, F. O'Sullivan, 2015 MITEI Associate Member Symposium—storage, Renewables and the Evolution of the Grid, 2016.
- [16] FERC, Settlement Intervals and Shortage Pricing in Markets Operated by Regional Transmission Organizations and Independent System Operators, 2016 [ONLINE] Available at: <https://www.ferc.gov/whats-new/comm-meet/2016/061616/E-2.pdf> (Accessed 4 August 16).
- [17] U.S. Department of Energy, DOE Global Energy Storage Database, 2012. <http://www.energystorageexchange.org/> (Accessed 30 August 16).
- [18] D. Bernardi, E. Pawlikowski, J. Newman, A general energy balance for battery systems, *J. Electrochem. Soc.* 132 (1985) 5–12.
- [19] L. Rao, J. Newman, Heat-generation rate and general energy balance for insertion battery systems, *J. Electrochem. Soc.* 144 (1997) 2697–2704.
- [20] W. Fang, O.J. Kwon, C.-Y. Wang, Electrochemical-thermal modeling of automotive Li-ion batteries and experimental validation using a three-electrode cell, *Int. J. Energy Res.* 34 (2010) 107–112.
- [21] T.F. Fuller, M. Doyle, J. Newman, Simulation and optimization of the dual lithium ion insertion cell, *J. Electrochem. Soc.* 141 (1994) 1–10.
- [22] M. Doyle, T.F. Fuller, J. Newman, Modeling of galvanostatic charge and discharge of the lithium/polymer/insertion cell, *J. Electrochem. Soc.* 140 (1993) 1526–1533.
- [23] M. Doyle, J. Newman, A.S. Gozdz, C.N. Schmutz, J. Tarascon, Comparison of modeling predictions with experimental data from plastic lithium ion cells, *J. Electrochem. Soc.* 143 (1996) 1890–1903.
- [24] P. Arora, M. Doyle, R.E. White, Mathematical modeling of the lithium deposition overcharge reaction in lithium-ion batteries using carbon-based negative electrodes, *J. Electrochem. Soc.* 146 (1999) 3543–3553.
- [25] L. Song, J.W. Evans, Electrochemical-thermal model of lithium polymer batteries, *J. Electrochem. Soc.* 147 (2000) 2086–2095.
- [26] W.B. Gu, C.Y. Wang, Thermal-electrochemical modeling of battery systems, *J. Electrochem. Soc.* 147 (2000) 2910–2922.
- [27] A.J. Bard, L.R. Faulkner, *Electrochemical Methods: Fundamentals and Applications* 2nd Edition, John Wiley & Sons, 2001, p. 52.
- [28] T.F. Fuller, M. Doyle, J. Newman, Simulation and optimization of the dual lithium ion insertion cell, *J. Electrochem. Soc.* 141 (1) (1994) 1–10.
- [29] D. Dees, E. Gunen, D. Abraham, A. Jansen, J. Prakash, Electrochemical modeling of lithium-ion positive electrodes during hybrid pulse power characterization tests, *J. Electrochem. Soc.* 155 (8) (2008) A603–A613.
- [30] D. Stephenson, S. Kim, F. Chen, E. Thomsen, V. Viswanathan, W. Wang, V. Sprenkle, *J. Electrochem. Soc.* 159 (12) (2012) A1993.
- [31] W.R. McKinnon, *Physics Mechanisms of Intercalation Batteries*, Thesis, Department of Physics, University of British Columbia, 1980, p. 37.
- [32] A.J. Bard, L.R. Faulkner, *Electrochemical Methods: Fundamentals and Applications* 2nd Edition, John Wiley & Sons, 2001, p. 99.
- [33] K.G. Gallagher, P.A. Nelson, D.W. Dees, Simplified calculation of the area specific impedance for battery design, *J. Power Sources* 196 (2011) 2289–2297.
- [34] R. Darling, K.G. Gallagher, J. Kowalski, S. Ha, F. Brushett, Pathways to low-cost electrochemical energy storage: a comparison of aqueous and nonaqueous flow batteries, *Energy & Environ. Sci.* 7 (11) (2014) 3459–3477.
- [35] R.L. Burwell Jr., R.G. Pearson, "The principle of microscopic reversibility, *J. Phys. Chem.* 70 (1) (1966) 300–302.
- [36] A. Sakti, J.J. Michalek, S.-E. Chun, J.F. Whitacre, *Int. J. Energy Res.* 37 (12) (2013) 1562–1568.
- [37] R. Sioshansi, P. Denholm, T. Jenkin, J. Weiss, Estimating the value of electricity storage in PJM: arbitrage and some welfare effects, *Energy Econ.* 31 (2009) 269–277.
- [38] N. Lu, J.H. Chow, A.A. Desrochers, Pumped-storage hydro-turbine bidding strategies in a competitive electricity market, *IEEE Trans. Power Syst.* 19 (2) (2004) 834–841.